Left ventricular pumping during the transition–adaptation sequence in preterm infants: impact of the patent ductus arteriosus

Sigrid Baumgartner[1], Monika Olischar[1], Martin Wald[2], Tobias Werther[1], Angelika Berger[1], Thomas Waldhör[3], Georg Fischer[4] and Ulrike Salzer-Muhar[5]

BACKGROUND: Postnatally, the immature left ventricle (LV) is subjected to high systemic afterload. Hypothesizing that LV pumping would change during transition–adaptation, we analyzed the LV in preterm infants (GA ≤ 32+6), clinically stable or with a hemodynamically significant patent ductus arteriosus (hPDA) by applying a pump model.

METHODS: Pumping was characterized by E_A (effective arterial elastance, reflecting afterload), E_{ES} (end-systolic LV elastance, reflecting contractility), E_A/E_{ES} coupling ratios, descriptive E_A:E_{ES} relations, and E_A/E_{ES} graphs. Data calculated from echocardiography and blood pressure were analyzed by diagnosis (S group: clinically stable, no hPDA, $n = 122$; hPDA group, $n = 53$) and by periods (early transition: days of life 1–3; late transition: 4–7; and adaptation: 8–30).

RESULTS: *S group*: LV pumping was characterized by an increased E_A/E_{ES} coupling ratio of 0.65 secondary to low E_{ES} in early transition, a tandem rise of both E_A and E_{ES} in late transition, and an E_A/E_{ES} coupling ratio of 0.45 secondary to high E_{ES} in adaptation; *hPDA group*: time-trend analyses showed significantly lower E_A ($P < 0.0001$) and E_{ES} ($P = 0.006$). Therefore, LV pumping was characterized by a lower E_A/E_{ES} coupling ratio ($P = 0.088$) throughout transition–adaptation.

CONCLUSIONS: In stable infants, facing high afterload, the immature LV, enhanced by the physiological PDA, increases its contractility. In hPDA, facing low afterload, the overloaded immature LV exhibits a consistently lower contractility.

In term infants, immediate cardiovascular transition at birth is followed by an early-transition phase (change from a right-to-left to a left-to-right shunt (LRS) across the patent ductus arteriosus (PDA)), a late-transition phase (oxygen-mediated PDA constriction by days of life 2–3), and eventually, an adaptation phase (at the end of the first and subsequent weeks of life (left ventricular and vascular remodeling) (1).

In preterm infants, this physiological cardiovascular transition–adaptation sequence has to proceed with altered responses in the systemic and pulmonary vasculature (2,3). While individual infants will exhibit near-to-physiologic hemodynamics within a slightly prolonged sequence, others will exhibit pathophysiologic hemodynamics, such as a hemodynamically significant PDA (hPDA) with cardiac and pulmonary volume overload (4,5), as well as altered cerebral perfusion (6).

The left ventricle (LV) of the preterm infant has to pump an appropriate stroke volume (SV) while being prematurely exposed to a high systemic afterload. According to published knowledge, the immature LV exhibits an inherently low contractility and a particular sensitivity to increases in afterload (7).

The Immature LV

Before birth, the fetal LV pumps into the aorta up to the watershed of the isthmus, its two respective sources of filling being the foramen ovale and the pulmonary blood flow. In the sarcomere, the fetal isoform of titin is less stiff than the postnatal form (7). The giant myofilament protein titin is the largest protein known and spans a continuous filament network across the sarcomere. Titin, by acting as a molecular spring, defines the passive elasticity of the cardiomyocyte in diastole (8). The compliant fetal titin isoform enables the heart to grow and to generate an adequate output even at the very low filling pressures *in utero* (7,9).

In late gestation, an inverse correlation between foramen ovale shunt flow and pulmonary blood flow has been noted (10). It is very likely that the augmentation of pulmonary blood flow (reaching up to 30% of the combined ventricular output) is driven by variations in pulmonary vascular resistance (10).

Concomitantly, both the increasing LV Doppler early diastolic filling rates (11) and decreasing isovolumetric

[1]Department of Pediatrics and Adolescent Medicine, Division of Neonatology, Pediatric Intensive Care and Neuropediatrics, Medical University of Vienna, Vienna, Austria; [2]Department of Pediatrics and Adolescent Medicine, Division of Neonatology, Paracelsus Medical University, Salzburg, Austria; [3]Department of Epidemiology, Medical University of Vienna, Vienna, Austria; [4]Section for Medical Information Management and Imaging, Medical University of Vienna, Austria; [5]Department of Pediatrics and Adolescent Medicine, Division of Pediatric Cardiology, Medical University of Vienna, Vienna, Austria. Correspondence: U Salzer-Muhar (ulrike.salzer@meduniwien.ac.at)

Received 11 September 2017; accepted 5 February 2018; advance online publication 11 April 2018. doi:10.1038/pr.2018.22

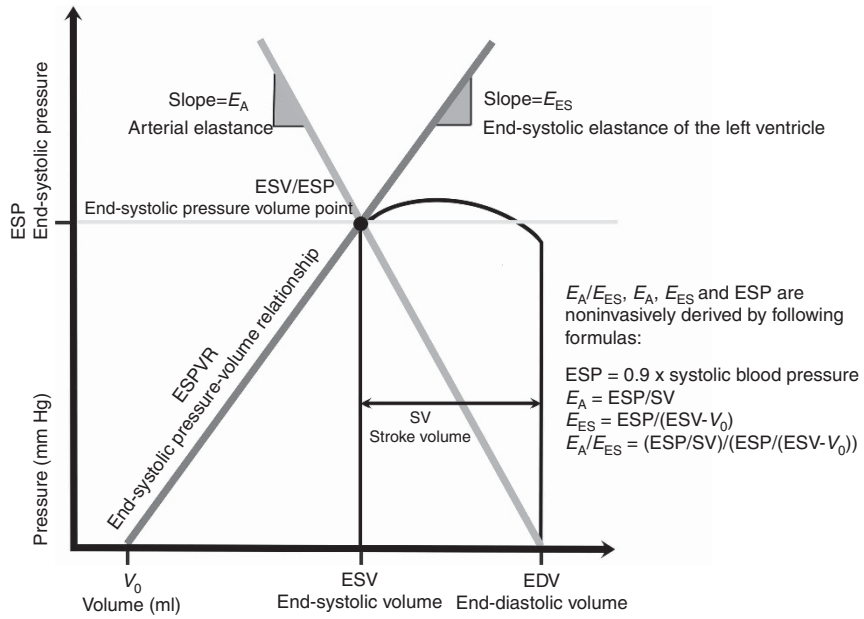

Figure 1. Pressure–volume relationship. Arterial elastance (E_A) is a measure of left ventricle (LV) afterload and is the slope of the line passing the *x* axis intercept end-diastolic volume (EDV) and the end-systolic volume (ESV)/end-systolic pressure (ESP) point. ESP volume relation (ESPVR) provides a load-independent measure of contractile function and is defined by the slope E_{ES} and V_0. E_{ES} quantifies LV elastance at the end systole.

relaxation time (12) indicate an improvement in relaxation and subsequently an increased LV preload.

An increased preload enhances systolic performance and thus SV. This is known as the Frank–Starling mechanism. In the sarcomere, it is again the giant myofilament protein titin that governs this mechanism (8). By regulating the length of the thick myosin filament, titin defines muscular force and how this force varies with muscle length (13).

The stiff postnatal titin isoform promotes, and the compliant fetal titin isoform attenuates the Frank–Starling mechanism (8). With term birth, the LV will be already prepared to pump an appropriate SV. With preterm birth, however, the lack of late gestation filling and the presence of the fetal titin isoform could attenuate the systolic function of the immature, inadequately preloaded LV.

As we hypothesized that the systolic pump function of the immature LV would change during transition–adaptation, we set up this study to explore the LV throughout this unique period. To include the effect of physiological and pathophysiological ductal patency on afterload, we searched for a method that would enable us to assess the LV, and concomitantly, its systemic afterload in preterm infants.

Ventricular–Arterial Coupling

The theoretical pump model ventricular–arterial coupling (E_A/E_{ES}) of Sunagawa *et al.* (14) allows analysis of the systolic pump function of the LV in its context to the arterial system (15). While E_A, effective arterial elastance, characterizes the net afterload, E_{ES}, end-systolic chamber elastance, is a load-independent descriptor of LV contractility that is also influenced by LV geometry, end-systolic stiffness, and myocardial properties (16,17).

The gold standard for estimating the components E_A and E_{ES} is the invasively obtained pressure–volume relationship (**Figure 1**, a modified version of Chantler *et al.* (18)). E_A can be derived by the end-systolic pressure (ESP)–stroke–volume relationship and E_{ES} by the ESP–volume relationship. Invasive evaluation is not feasible in the fragile patient group of preterm infants. However, the sophisticated and diverse methodology (18–21) to estimate LV pump function from echocardiographic parameters (end-systolic volume (ESV), SV, and from blood pressure (BP)) that has already been applied in both adults (17,22) and children (19,20,23,24) appeared to be a noninvasive alternative for preterm infants.

We decided to use the E_A/E_{ES} model to explore the systolic pump function of the immature ventricle during transition–adaptation. The aim of this study was to assess LV pumping during the transition–adaption sequence in stable preterm infants with near-to-physiologic hemodynamics and also in sick infants exhibiting the pathophysiologic hemodynamics of a hPDA.

METHODS

We used data collected for a prospective study on PDA treatment. Examinations were performed following our functional Echocardiography (fEcho) Protocol established in 2009, which is in line with published recommendations (25). Our setting of fEcho also includes prospectively standardized electronic fEcho Report Forms that ensure automatic insertion of the infants' demographic data, heart rate, BP, and oxygen saturation at the moment of examination. Drop downs allow linking of measurements immediately to preterm-relevant hemodynamics. Report forms, images, and loops are archived in our fEcho Digital Platform (created by the Section for Medical Information Management and Imaging by the Medical University of Vienna, Austria).

Study Population

The inclusion criteria were very preterm infants born between 23+0 and 32+6 weeks of gestation, diagnosis of near-to-physiologic hemodynamics or hPDA, and normal intracardiac anatomy.

We formed groups by diagnosis: (i) *hPDA group*: a pure LRS across the PDA and an end-diastolic flow velocity in the left pulmonary artery (LPAd) ≥ 0.2 m/s (4), which—with normal-sized pulmonary arteries—indicates a significant LRS into the pulmonary vasculature. (ii) *S group*: clinically stable, with either a closed PDA or a non-hPDA (LPAd < 0.2 m/s, ratio of the left atrial diameter to the aortic diameter < 1.4, and no abdominal aortic backward flow (5)).

To represent the phases of the transition–adaptation sequence, we split the results within each group by periods based on the days of life (DOL) on which the examinations were performed: period 1: DOL 1–3 (early transition), period 2: DOL 4–7 (late transition), and period 3: DOL 8–30 (adaptation). By defining those time frames, which slightly exceeded the established term infants' time frames, we aimed to take into account the assumed prolongation of the transition–adaptation sequence in preterm infants.

If infants had more than one examination in one period, we only included the first examination.

Data

Weight, heart rate, transcutaneous oxygen saturation, and BP (measured invasively if a catheter was in place) were retrieved from electronic fEcho Report Forms. BP was measured invasively if a catheter was in place or noninvasively.

End-diastolic volume (EDV), ESV, and SV were retrieved from the fEcho Digital Platform. These volumes, based on M-mode measurements of the end-diastolic and end-systolic diameters of the LV (parasternal long axis view) are provided by the software of the ultrasound machine (Siemens, Acuson S2000) using the Teichholz formula (26).

LV Systolic Pump Function

Regarding E_A and E_{ES} and the so-called E_A/E_{ES} coupling ratio, we refer to **Figure 1** (18). To apply the pump model and its formulas which were developed for adults (14) in preterm infants, we estimated E_A, E_{ES}, and ESP by the following formulas: ESP = 0.9 × systolic BP (20,27,28); E_A = ESP/SV (14); and E_{ES} = ESP/(ESV−V_0). V_0 is the left ventricular volume at a theoretical (nonphysiological) ESP in the LV of 0 mm Hg (29,30). If we assume that V_0 is small compared with ESV (18), then V_0 might be neglected, and the calculation of E_{ES} reduces to E_{ES} = ESP/ESV (18–20).

The following approach-related limitations have to be considered:

(i) BP data included not only invasive measurements but also noninvasive measurements. The degree of agreement between the two methods may vary, but there may be substantial differences in individual preterm infants (31). This is also depicted by our own preliminary data obtained from 369 preterm infants with 918 examinations (**Supplementary Figure S1 (online)**, T. Werther *et al.*).

(ii) Calculation of ESP by 0.9 × systolic BP may slightly underestimate the ESP subject to the contour of the individual LV pressure curve in the hPDA group.

(iii) The Teichholz method overestimates both EDV and ESV, and thus leads to a significantly higher SV compared with SVs calculated by other methods (28,32). Aiming to compare E_A, E_{ES}, and E_A/E_{ES} between groups, we considered this systematic bias as being acceptable. In premature infants, obtaining a true apical four-chamber view for LV volumetric chamber quantification is not always feasible.

(iv) In a recent validation study performed in children with near-to-normal loading conditions, 3D echocardiographic estimated E_{ES} correlated best with invasively measured E_{ES} when V_0 was neglected (20). This was attributed to the high interobserver variability in the measurement of the pre-ejection period (required for the calculation of V_0) in the presence of high heart rates. In hPDA pathophysiology, however, when V_0 is increased, neglecting of V_0 may lead to underestimation of E_{ES} and consecutively, to overestimation of E_A/E_{ES}.

(v) The E_A/E_{ES} graphs (**Figure 2**) were drawn by using the equation of a straight line (ESP = E_{ES} × ESV+d_{Ees} and ESP = E_A × ESV+d_{Ea}). The mean values of E_{ES}, E_A, and the ESP volume point (ESP/ESV) were used to calculate d (d_{Ees} and d_{Ea}) and to draw the straight lines. Thus, the E_A/E_{ES} graphs represent the mean values for E_A, E_{ES}, and ESP/ESV, whereas V_0 and EDV result from the respective x axis intercepts of the two lines.

Statistics

Mean values and standard deviation were used to describe infants' characteristics including clinical and echocardiographic parameters, as well as E_A, E_{ES}, and E_A/E_{ES}.

The effects of the variables "diagnosis" and "period" on E_A, E_{ES}, and E_A/E_{ES} were estimated by means of a linear mixed model in SAS (SAS VS. 9.4 Institute Inc., Cary, NC, 2012). The variables "diagnosis" and "period" were treated as class effects. The *a priori* null hypothesis of the equality of time trends between the two diagnosis groups was tested using an interaction term diagnosis × period. E_A, E_{ES}, and E_A/E_{ES} were transformed using the natural logarithm to approach a normal residual distribution. The significance level was set to 0.05/3 by means of the Bonferroni correction to adjust for multiple testing by estimating three regression models.

Ethics

This study (EC-no. 1079/2011) and also the prospective study on PDA treatment (EC-no. 875/2010) were approved by the Ethics Board of the Medical University of Vienna.

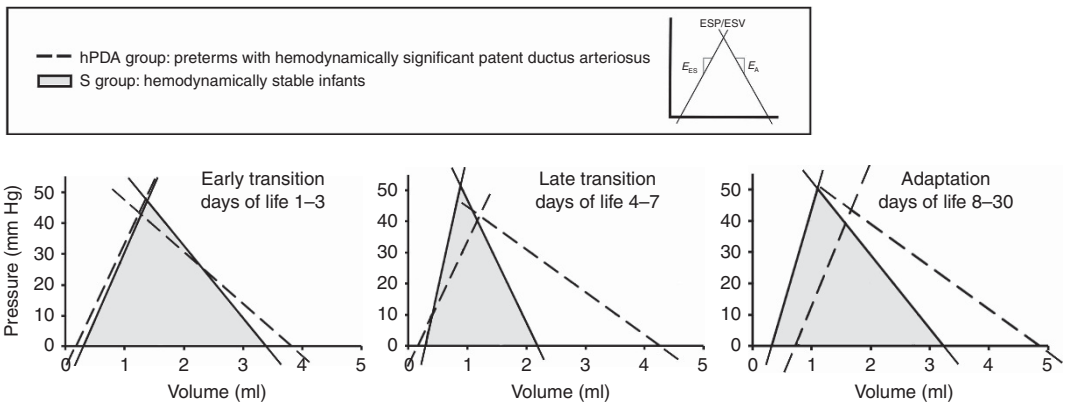

Figure 2. Comparison of the corresponding ventricular–arterial coupling (E_A/E_{ES}) graphs.

RESULTS

The study population included 126 preterm infants with a total number of 175 echocardiographic examinations, of which 122 were assigned to the S group and 53 to the hPDA group. Actually, 40 preterm infants had multiple observations, 4 preterm infants crossed from the hPDA group to the S group, and 12 patients in the hPDA group had serial measurements.

Table 1. Clinical and echocardiographic parameters of the S and hPDA group

	S group, $n = 122$			hPDA group, $n = 53$		
	DOL 1–3, $n = 30$	DOL 4–7, $n = 63$	DOL 8–30, $n = 29$	DOL 1–3, $n = 19$	DOL 4–7, $n = 18$	DOL 8–30, $n = 16$
			Demographic data			
Current weight (g)	1,043 ± 249	1,057 ± 249	1,157 ± 294	1,018 ± 286	880 ± 273	1,049 ± 376
			Vital parameters at the time of echocardiographic examination			
Saturation (%)	90 ± 20	95 ± 3	93 ± 4	91 ± 4	93 ± 4	92 ± 7
Heart rate (b.p.m.)	152 ± 12	152 ± 13	160 ± 14	153 ± 12	154 ± 11	162 ± 17
Blood pressure (mm Hg)	52/29 ± 8/7	57/33 ± 10/8	56/28 ± 9/7	48/26 ± 7/6	46/25 ± 7/5	48/25 ± 7/6
			Echocardiographic measurements			
Stroke volume (ml)	2.3 ± 1.0	2.2 ± 1.0	2.5 ± 1.0	2.9 ± 1.5	3.5 ± 1.4	4.1 ± 2.1
Stroke volume (ml/kg)	2.2 ± 0.8	2.1 ± 0.8	2.3 ± 0.8	2.9 ± 1.8	4.0 ± 1.2	3.9 ± 1.2
End-systolic volume (ml)	1.4 ± 0.7	0.9 ± 0.5	1.1 ± 0.7	1.3 ± 0.6	1.2 ± 0.6	1.7 ± 1.6
Fractional shortening (%)	31 ± 7	37 ± 11	38 ± 11	37 ± 10	39 ± 4	40 ± 9

DOL, days of life; hPDA, hemodynamically significant patent ductus arteriosus; S, stable preterms.

Table 2. Comparison of E_A/E_{ES}, E_A, and E_{ES} between the S and hPDA group

	S group, $n = 122$			hPDA group, $n = 53$			*P* values type III tests of fixed effects	
	DOL 1–3 $n = 30$	DOL 4–7 $n = 63$	DOL 8–30 $n = 29$	DOL 1–3 $n = 19$	DOL 4–7 $n = 18$	DOL 8–30 $n = 16$	Diagnosis	Period
E_A/E_{ES}	0.65 ± 0.42	0.56 ± 0.61	0.45 ± 0.29	0.49 ± 0.35	0.35 ± 0.09	0.39 ± 0.21	0.0876	0.0582
E_A (mm Hg/ml)	24 ± 10	40 ± 50	24 ± 10	17 ± 8	14 ± 6	14 ± 7	< .0001	0.2517
E_{ES} (mm Hg/ml)	44 ± 26	85 ± 81	65 ± 39	40 ± 15	40 ± 18	46 ± 33	0.0062	0.0425

DOL, days of life; E_A, arterial elastance; E_A/E_{ES}, ventricular–arterial coupling; E_{ES}, end systolic elastance of the left ventricle; hPDA, hemodynamically significant patent ductus arteriosus; S, stable preterms.

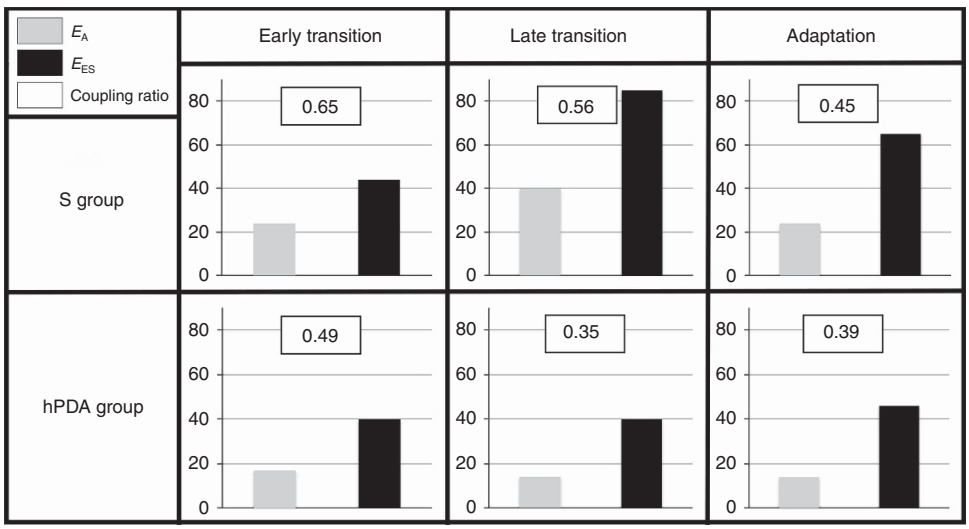

Figure 3. Ventricular–arterial coupling (E_A:E_{ES}) relations and their changes during transition–adaptation.

A non-hPDA was present in the S-group at 67%, 46%, and 10% in the periods 1, 2, and 3, respectively.

Comparison of the S Group vs. the hPDA Group

Table 1 presents descriptive statistics of clinical and echocardiographic parameters in the two groups. Oxygen saturation (except in period 1), and systolic and diastolic BP were lower in the hPDA group.

Table 2 shows results of the comparison of E_A/E_{ES}, E_A, and E_{ES}. The interaction term diagnosis × period, being not significant, indicated a lack of effect of period between the two groups. E_{ES} ($P = 0.0062$) and E_A ($P < 0.0001$) were significantly lower in the hPDA group, whereas E_A/E_{ES} was not.

Descriptive Analysis. *S group*: E_A was comparable in periods 1 and 3. E_{ES} was at minimum in period 1. E_A/E_{ES} coupling ratios show a gradual decrease with 0.65 in period 1, 0.56 in period 2, and 0.45 in period 3 (Figure 3).

hPDA group: E_A was consistently low in periods 1, 2, and 3. E_{ES}, comparable to the minimum of E_{ES} in the S group, was low in periods 1 and 2, and at its maximum in period 3. E_A/E_{ES} coupling ratios were 0.49 in period 1, 0.35 in period 2, and 0.39 in period 3, respectively.

E_A/E_{ES} Graphs. The corresponding E_A/E_{ES} graphs (Figure 2) for the S group showed higher ESP levels (due to higher systolic BP), whereas the corresponding E_A/E_{ES} graphs for the hPDA group showed an expansion and a rightward shift due to low E_A and E_{ES} (resulting from high SV and ESV values).

DISCUSSION

Advantages of the E_A/E_{ES} Pump Model

There are two reasons why we chose the E_A/E_{ES} pump model to analyze LV systolic pump function within the transition–adaptation sequence:

First, the E_A/E_{ES} coupling ratio is inversely related to the ejection fraction ($E_A/E_{ES} = 1/$ (ejection fraction-1)) with the additional advantage that by examining E_A and E_{ES} separately, alterations can be attributed to alterations in arterial or ventricular function, or both (18). Generally, E_{ES} is matched with E_A, and more specifically, E_{ES} responds to a given E_A. Various conditions, however, may lead to an acute mismatch between the arterial and ventricular systems (18). During exercise for example, a disproportionate increase occurs in E_{ES} vs. E_A due to an increase in left ventricular output caused by the higher speed and force of the left ventricular contractility (17). Corresponding to this acute mismatch, the E_A/E_{ES} coupling ratio decreases.

Second, the E_A/E_{ES} coupling ratio describes cardiac energetics. The efficiency of the ventricle as a pump is defined by the ratio between mechanical work (stroke work) and energy consumption (amount of oxygen the LV consumes while performing stroke work) (33). In adults, maximal energetic efficiency occurs when the E_A/E_{ES} coupling ratio is close to 0.5 and maximal efficacy (stroke work) occurs when E_A/E_{ES} coupling ratio is close to 1.0 (10, 13). In adults at rest, an optimal E_A/E_{ES} coupling ratio between 0.7 and 1 seems to reflect the optimal balance between stroke work and energy consumption (17).

Before interpreting our results, we would like to point out that in children, due to smaller vessels and a higher heart rate, numeric values for E_A and E_{ES} are higher (17). They are inversely related to the body surface area (34). As E_{ES} values are by proportion higher in children than in adults, numeric E_A/E_{ES} coupling ratios are lower. Published estimates for E_A/E_{ES} coupling ratios are 0.7 (34) and 0.6 (24) in children, and 0.5 in term infants, respectively (23).

Estimated E_A/E_{ES} Coupling Ratios in the Periods of the Transition–Adaptation Sequence

In stable preterm infants, we observed a gradual decrease of estimated E_A/E_{ES} from 0.65 in early transition over 0.56 in late transition to 0.45 in adaptation. We think that defining the three periods by the chosen time frames might have contributed to the nonsignificance of these results, as the length of these periods may vary individually.

The result, however, proved our hypothesis. It implies that in stable preterm infants with near-to-physiologic hemodynamics, the systolic pump function of the immature LV changes within the phases of the physiological transition–adaptation sequence. Besides, the value of 0.45 in adaptation, due to a proportionally even higher E_{ES} (Figure 3), corresponds well to the reported estimates in children.

With respect to the aforementioned cardiac energetics, the observed gradual decrease of the E_A/E_{ES} coupling ratios indicates that in near-to-physiologic hemodynamics, the immature LV performs high stroke work in early transition and becomes more energy-efficient toward adaptation.

In preterm infants with hPDA, the consistently, albeit not significantly lower E_A/E_{ES} coupling ratios throughout all periods may indicate a shift toward more LV energy efficiency (in response to the increased oxygen demand of the myocardium) at the expense of stroke work (15,33). Our results are in line with the significantly lower E_A/E_{ES} coupling ratios found (using a different methodology and definition of the PDA profile) in a recent study in preterm infants with an at least 14 days of exposure to a PDA (28).

E_A:E_{ES} Relations in the Three Periods of the Transition–Adaptation Sequence

Examining E_A:E_{ES} relations (Table 2 and Figure 3) and E_A/E_{ES} graphs (Figure 2) provided comprehensive insight into LV pumping in the respective days of life.

Stable preterm infants. In early transition, LV pumping was characterized by a maximum E_A/E_{ES} coupling ratio secondary to a low E_{ES}. A non-hPDA was present in 67% of these infants.

Our findings are in line with published data. They confirm that in this period, BP is kept up by the high systemic vascular resistance and not by SV (35), and also that the contractility of the immature myocardium is inherently low (7).

In late transition, LV pumping was characterized by a tandem rise of E_A and E_{ES}. The PDA was already closed in 54% of these infants. Higher E_A, due to a higher systolic BP, indicated a higher afterload. E_{ES} was higher due to better contractility (36) and altered the LV geometry (**Figure 2**). The observed tandem rise indicates better LV contractility in response to the increased afterload. The concomitantly observed change in LV geometry, however, could also signify a transient ventricular–vascular stiffening with the cessation of the ductal LRS. So far, an increase of E_A and E_{ES} due to ventricular and vascular stiffening has been described only with age-related changes of the LV and the arterial system (16,22,37).

In adaptation, LV pumping was characterized by a lower E_A/E_{ES} coupling ratio secondary to high E_{ES}. In comparision to late transition, lower E_A, numerically comparable to period 1, resulted more from higher SV than from lower BP. The PDA was closed in 90% of these infants. Lower E_{ES} compared with late transition was due to higher ESV and very likely indicated lower LV stiffness. The immature LV was remodeled.

Preterm infants with hPDA. In early transition, LV pumping was characterized by a lower E_A/E_{ES} coupling ratio than in stable infants. This was secondary to low E_A and E_{ES} and confirms recent literature (28). E_A, due to lower systolic BP and higher SV in hPDA (5), was significantly lower throughout transition–adaptation as was E_{ES}, reflecting lower contractility and changed geometry of the volume-loaded LV. Accordingly, the E_A/E_{ES} graph in adaptation (**Figure 2**) represents a marked rightward shift of the curve, as described in adult patients with heart failure (29,30).

We would like to point out that, as already acknowledged in the Methods section, we might have underestimated E_{ES} by neglecting the increasing V_0 in late transition and adaptation. To prevent this would have required measurement of the pre-ejection period, which has a poor interobserver repeatability in preterm infants, despite an overall good correlation in adults (38).

E_A/E_{ES} graphs (**Figure 2**) and the corresponding E_A:E_{ES} relation (**Figure 3**) enhance our understanding of the pathophysiology of the post ligation cardiac syndrome (39,40), where the increased afterload, cessation of the LRS, and lowered LV preload lead to an acute E_A:E_{ES} relation mismatch. Serial postoperative E_A and E_{ES} calculations, also estimated using the Teichholz methodology, revealed that E_{ES} improves faster than E_A after ligation of the PDA (41).

LV Pumping and the PDA

We consider the noticed high E_A/E_{ES} coupling ratio secondary to a low E_{ES} in early transition and the consecutive tandem rise of both E_A and E_{ES} in late transition in stable preterm infants to be the most interesting result of this study. The corresponding E_A/E_{ES} graphs (**Figure 2**) and the unexpectedly small variation in the SV/kg (**Table 1**) led us to conclude that physiological ductal patency, specifically the LRS in early and late transition, very likely enhances the augmentation of E_{ES} in late transition.

Actually, the LRS across the PDA causes a slight overperfusion of the entire fetal "minor" circulation extending from the pulmonary branches to the aortic isthmus, and concomitantly, it reduces systemic afterload. The PDA adds to pulmonary perfusion, and its highly oxygen-saturated blood and also vascular stretch reduce pulmonary vascular resistance. In term infants, the increased pulmonary venous return enhances closure of the preexisting second LV-filling source, the foramen ovale, and increases filling of the mature, after late gestation already adequately preloaded LV. Eventually, by the Frank–Starling mechanism, this increased LV preload increases LV contractility. The resulting augmented SV in the aorta proximal to the watershed of the isthmus is also beneficial for coronary and cerebral perfusion (42).

In preterm infants with less mature lungs, a less restrictive foramen ovale and an inadequately preloaded LV that described slight overperfusion seems to be of an even greater relevance. This training enables the immature LV to exhibit an adequate contractility (E_{ES}) when being subjected to the increase in E_A associated with ductal constriction.

All this, however, applies only to near-to-physiologic hemodynamics, but not to pathophysiologic hemodynamics when a large LRS across the PDA causes LV overload (**Figure 2**) and—by overperfusion—sometimes hemorrhagic pulmonary edema and cerebral hemorrhage (40).

Our conclusion that physiological ductal patency in transition is very likely a key factor for the evolution of LV pumping toward better contractility during transition–adaptation is based on the principles of the Frank–Starling mechanism. As explained in the introduction, the regulator of this mechanism in the sarcomere is titin (8,13). Further research is needed on titin and its respective isoform myocardial expression rates in both term and preterm infants in this unique period.

There are inherent limitations of our study. This was a retrospective study without preemptive sample size calculations. Thus, nonsignificant P values do not necessarily point to the absence of an effect under consideration. A point of criticism could be our methodological approach to which we have referred in detail in the Methods section. The classification by period was largely based on term infants' time frames for transition and adaptation, which may vary individually in very preterm infants. The strengths of the study include the sample size, the well-elaborated and structured setting of fEcho in our NICU with continuous computerization and simultaneously measured vital parameters, experienced examiners ensuring reliable, high-quality data, as well as the fact that by the retrospective design, examiners were unbiased when analyzing E_A and E_{ES}.

CONCLUSION

The immature LV faces an increase of afterload after birth. We analyzed the systolic pump function of the immature LV in a cohort of very preterm infants within the transition–

adaptation sequence by applying the E_A/E_{ES} pump model in which E_A reflects the net afterload, whereas E_{ES} reflects the foremost contractility.

In stable preterm infants with near-to-physiologic hemodynamics, LV systolic pump function was characterized by a maximum E_A/E_{ES} coupling ratio secondary to low E_{ES} in early transition, a tandem rise of E_A and E_{ES} in late transition, and a low E_A/E_{ES} coupling ratio secondary to high E_{ES} in adaptation. These findings lead us to conclude that LV pumping evolves toward higher contractility and also that this process is enhanced by the physiological PDA.

In preterm infants with the pathophysiologic hemodynamics of a hPDA, LV systolic-pump function was characterized by significantly lower E_A and lower E_{ES} throughout transition–adaptation. These findings add to the understanding of the postligation syndrome when the immature overloaded LV faces an abrupt rise in systemic afterload with cessation of the PDA.

SUPPLEMENTARY MATERIAL

Supplementary material is linked to the online version of the paper at http://www.nature.com/pr

ACKNOWLEDGMENTS

We thank Dave Hill for his valuable assistance in preparation of this manuscript.

Disclosure: The authors declare no conflict of interest.

REFERENCES

1. Azhibekov T, Soleymani S, Lee BH, et al. Hemodynamic monitoring of the critically ill neonate: an eye on the future. Semin Fetal Neonatal Med 2015;20:246–54.
2. Engle WD. Blood pressure in the very low birth weight neonate. Early Hum Dev 2001;62:97–130.
3. Noori S, Seri I. Pathophysiology of newborn hypotension outside the transitional period. Early Hum Dev 2005;81:399–404.
4. El Hajjar M, Vaksmann G, Rakza T, et al. Severity of the ductal shunt: a comparison of different markers. Arch Dis Child Fetal Neonatal Ed 2005;90:F419–22.
5. Jain A, Shah PS. Diagnosis, evaluation, and management of patent ductus arteriosus in preterm neonates. JAMA Pediatr 2015;169:863–72.
6. Evans N, Kluckow M. Early ductal shunting and intraventricular haemorrhage in ventilated preterm infants. Arch Dis Child Fetal Neonatal Ed 1996;75:F183–6.
7. Finnemore A, Groves A. Physiology of the fetal and transitional circulation. Semin Fetal Neonatal Med 2015;20:210–6.
8. Hamdani N, Herwig M, Linke WA. Tampering with springs: phosphorylation of titin affecting the mechanical function of cardiomyocytes. Biophys Rev 2017;9:225–37.
9. Walker JS, de Tombe PP. Titin and the developing heart. Circ Res 2004;94:860–2.
10. Prsa M, Sun L, van Amerom J, et al. Reference ranges of blood flow in the major vessels of the normal human fetal circulation at term by phase-contrast magnetic resonance imaging. Circ Cardiovasc Imaging 2014;7:663–70.
11. Fernandez Pineda L, Tamariz-Martel Moreno A, Maitre Azcarate MJ, et al. Contribution of Doppler atrioventricular flow waves to ventricular filling in the human fetus. Pediatr Cardiol 2000;21:422–8.
12. Bhorat I, Bagratee J, Reddy T. Gestational age-adjusted trends and reference intervals of the Modified Myocardial Performance Index (Mod-MPI) and its components, with its interpretation in the context of established cardiac physiological principles. Prenat Diagn 2014;34:1031–6.
13. Tonino P, Kiss B, Strom J, et al. The giant protein titin regulates the length of the striated muscle thick filament. Nat Commun 2017;8:1041–9.
14. Sunagawa K, Maughan WL, Burkhoff D, et al. Left ventricular interaction with arterial load studied in isolated canine ventricle. Am J Physiol 1983;245:H773–80.
15. Starling MR. Left ventricular–arterial coupling relations in the normal human heart. Am Heart J 1993;125:1659–66.
16. Borlaug BA, Kass DA. Ventricular–vascular interaction in heart failure. Heart Fail Clin 2008;4:23–36.
17. Chantler PD, Lakatta EG. Arterial–ventricular coupling with aging and disease. Front Physiol 2012;3:90.
18. Chantler PD, Lakatta EG, Najjar SS. Arterial–ventricular coupling: mechanistic insights into cardiovascular performance at rest and during exercise. J Appl Physiol (1985) 2008;105:1342–51.
19. Tanoue Y, Sese A, Ueno Y, et al. Bidirectional Glenn procedure improves the mechanical efficiency of a total cavopulmonary connection in high-risk fontan candidates. Circulation 2001;103:2176–80.
20. Chowdhury SM, Butts RJ, Taylor CL, et al. Validation of noninvasive measures of left ventricular mechanics in children: a simultaneous echocardiographic and conductance catheterization study. J Am Soc Echocardiogr 2016;29:640–7.
21. Chen CH, Fetics B, Nevo E, et al. Noninvasive single-beat determination of left ventricular end-systolic elastance in humans. J Am Coll Cardiol 2001;38:2028–34.
22. Kass DA. Age-related changes in venticular–arterial coupling: pathophysiologic implications. Heart Fail Rev 2002;7:51–62.
23. Taborsky HS. Arterial–Ventricular Coupling in Term Neonates and Infants up to 6 months, A Retrospective Data Analysis.. Vienna: Pediatric and Adolescence Medicine. Medical University of Vienna: Vienna, 2015: 69.
24. Engel J, Baumgartner S, Novak S, et al. Ventriculo-arterial coupling in children with Still's murmur. Physiol Rep 2014: 2.
25. de Boode WP, Singh Y, Gupta S, et al. Recommendations for neonatologist performed echocardiography in Europe: Consensus Statement endorsed by European Society for Paediatric Research (ESPR) and European Society for Neonatology (ESN). Pediatr Res 2016;80:465–71.
26. Teichholz LE, Kreulen T, Herman MV, et al. Problems in echocardiographic volume determinations: echocardiographic–angiographic correlations in the presence of absence of asynergy. Am J Cardiol 1976;37:7–11.
27. Kelly RP, Ting CT, Yang TM, et al. Effective arterial elastance as index of arterial vascular load in humans. Circulation 1992;86:513–21.
28. de Waal K, Phad N, Collins N, et al. Cardiac remodeling in preterm infants with prolonged exposure to a patent ductus arteriosus. Congenit Heart Dis 2017;12:364–72.
29. Ky B, French B, May Khan A, et al. Ventricular–arterial coupling, remodeling, and prognosis in chronic heart failure. J Am Coll Cardiol 2013;62:1165–72.
30. Burkhoff D. Pressure–volume loops in clinical research: a contemporary view. J Am Coll Cardiol 2013;62:1173–6.
31. Meyer S, Sander J, Graber S, et al. Agreement of invasive versus non-invasive blood pressure in preterm neonates is not dependent on birth weight or gestational age. J Paediatr Child Health 2010;46:249–54.
32. Nagasawa H, Kohno Y, Yamamoto Y, et al. Methodologic comparison of left ventricular stroke volumes in the early neonatal period by echocardiography. Pediatr Cardiol 2014;35:1415–20.
33. Burkhoff D, Sagawa K. Ventricular efficiency predicted by an analytical model. Am J Physiol 1986;250:R1021–7.
34. Khosroshahi HE, Ozkan EA, Kilic M. Arterial and left ventricular end-systolic elastance in normal children. Eur Rev Med Pharmacol Sci 2014;18:3260–6.
35. Pladys P, Wodey E, Beuchee A, et al. Left ventricle output and mean arterial blood pressure in preterm infants during the 1st day of life. Eur J Pediatr 1999;158:817–24.
36. Kluckow M, Evans N. Superior vena cava flow in newborn infants: a novel marker of systemic blood flow. Arch Dis Child Fetal Neonatal Ed 2000;82:F182–7.

37. Antonini-Canterin F, Carerj S, Di Bello V, et al. Arterial stiffness and ventricular stiffness: a couple of diseases or a coupling disease? A review from the cardiologist's point of view. Eur J Echocardiogr 2009;10:36–43.
38. Schwarz CE, Preusche A, Baden W, et al. Repeatability of echocardiographic parameters to evaluate the hemodynamic relevance of patent ductus arteriosus in preterm infants: a prospective observational study. BMC Pediatr 2016;16:18.
39. Noori S, McNamara P, Jain A, et al. Catecholamine-resistant hypotension and myocardial performance following patent ductus arteriosus ligation. J Perinatol 2015;35:123–7.
40. El-Khuffash A, Weisz DE, McNamara PJ. Reflections of the changes in patent ductus arteriosus management during the last 10 years. Arch Dis Child Fetal Neonatal Ed 2016;101:F474–8.
41. Nagata H, Ihara K, Yamamura K, et al. Left ventricular efficiency after ligation of patent ductus arteriosus for premature infants. J Thorac Cardiovasc Surg 2013;146:1353–8.
42. Noori SSI. The very low birth weight neonate with a hemodynamically significant ductus arteriosus during the first postnatal weekIn:Polin Reds. Hemodynamics and Cardiology. Neonatology Questions and Controversies 2nd edn. New York: Columbia University Medical Center, 2008: 269–91.